EFFECT OF PORE STRUCTURE ON ENERGY BARRIERS AND APPLIED VOLTAGE PROFILES

II. Unsymmetrical Channels

PETER C. JORDAN
Department of Chemistry, Brandeis University, Waltham, Massachusetts 02254

ABSTRACT This paper examines "realistic" pores, i.e., ones that are neither symmetric nor of uniform diameter. Methods are described that permit estimation of the image potential for an ion in an aqueous pore spanning a lipid membrane and for the electric field produced in such a pore when a transmembrane potential is applied. They are used to model features of the delayed rectifier potassium channel. Constraints on the geometry of the exterior mouth, the dielectric properties of the narrow part of the pore and the conduction mechanism are determined for this channel.

INTRODUCTION

In the previous paper (Jordan, 1984), I have analyzed the electrostatic properties of symmetrical, water-filled pores of nonuniform diameter spanning lipid-bilayer membranes. While a less artificial model of physiological channels than those presented in earlier work (Parsegian, 1969, 1975; Levitt, 1978; Jordan, 1981, 1982, 1983), it still is far from realistic. The available structural evidence for the acetylcholine receptor channel (Kistler and Stroud, 1981; Kistler et al., 1982), the delayed rectifier potassium channel (Armstrong, 1975 *a,b*; Hille, 1975) and the maxi-K channel (Miller, 1982; Latorre et al., 1982) indicates that biological pores are neither symmetric nor of constant cross section.

In this paper, I describe a method of estimating the electrostatic properties of channels that are "realistic" in the sense that their *cis* and *trans* geometries are different. Even with this extension, the model remains crude. No electrical distinction is made between the water bathing the membrane and that within the pore. The lipid and the pore former are described as a single electrical phase. The pore is assumed to have cylindrical symmetry.

I first demonstrate that for unsymmetrical channels, the electric field profile due to an applied voltage and the image potential for an ion on the pore axis can be approximated quite accurately from calculations on symmetrical channels. The analysis is then used to provide information about the structure and properties of the delayed rectifier potassium channel.

SPLICING METHOD

Applied Voltage Profiles

In the companion paper (Jordan, 1984), I showed that the potential profile in or external to a channel mouth is determined only by the nature of the source and the geometry of the mouth. As a result it is possible to estimate, with reasonable accuracy, potential profiles for unsymmetrical channels from calculations that describe symmetrical systems.

Consider applying a potential difference across an unsymmetrical model channel ensemble with the geometry illustrated in Fig. 1. From the treatment of symmetrical channels we know that (a) within the constriction the field is essentially constant and (b) the shape of the potental function on the left- and right-hand side of the constriction is determined by the respective mouth geometries. The properties of the asymmetrical channel can be established by dividing the system at a splice point S_0 and relating the properties of each half channel separately to those of the symmetrized halves. The obvious definition of S_0 is the point where the electric fields at the centers of both symmetrized half channels are the same. While in principle this is the simplest procedure, it requires finding a unique point of division. In practice the splice point can be chosen arbitrarily because the scaled fractional electrical distance function that describes the electric field outside the constricted region, as plotted in Fig. 9 of the preceding paper, depends only upon mouth geometry; it is totally independent of the length of the constriction. The method requires scaling the fields for the symmetrized halves.

The electric fields at the center of the symmetrized half channels are unequal for an arbitrary splice point. Fig. 2 *a* illustrates this for a moderately asymmetrical channel, $b_L = 5, \lambda = 15, b_R = 0$, contrasting two extreme choices of splice point, $d_s = 2.5$ and $d_s = 12.5$. If the voltage profile for each half channel is divided by the field, ϵ^0, at each channel center, a new profile is constructed for which the field within the constriction is constant. These profiles are continuous, but, as shown in Fig. 2 *b*, the potential change is from $+V_0/\mathcal{E}_L^0$ to $-V_0/\mathcal{E}_R^0$. The fractional electrical distance is now constructed by dividing each curve by the total voltage change, $V_0(-1/\mathcal{E}_R^0 - 1/\mathcal{E}_L^0) = -V_0(\mathcal{E}_L^0 + \mathcal{E}_R^0)/\mathcal{E}_L^0\,\mathcal{E}_R^0$, and shifting the abscissa of the resultant function by $\mathcal{E}_R^0/(\mathcal{E}_L^0 + \mathcal{E}_R^0)$; this ensures that the electrical distance varies from 0 to 1 as x varies from $-\infty$ to $+\infty$. These profiles are exhibited in Fig. 2 *c*. The functions are independent of the choice of splice point so that the correlation of fractional electrical distance with position is, for this geometry, essentially unambiguous. This is not generally the case. For highly asymmetric channels, the scaling procedure is less satisfactory. Fig. 2 also contrasts two choices of splice point for a geometry where $b_L = 10, \lambda = 10, b_R = 0$. A fractional electrical distance of 0.2 can only be said to be somewhere between 3.7 a_0 and 5.1 a_0 from the entrance to the channel mouth. Even so, the uncertainty is not too great. For a membrane 5.0 nm wide, a_0, given these parameters, is 0.25 nm; the corrresponding positional uncertainty is ±0.18 nm.

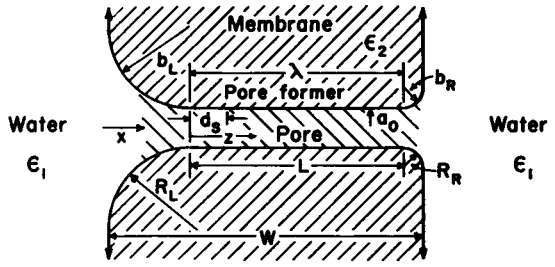

FIGURE 1 Cross section of an unsymmetrical pore spanning a membrane of width W. The radii of the *left*- and *right*-hand mouth openings are R_L and R_R, respectively, the pore length is L and its radius is a_0. When scaled by the pore radius, the structural parameters describing the model are $\lambda = L/a_0$, $b_L = R_L/a_0$, and $b_R = R_R/a_0$. The scaled distances from the entrance to the *left* hand mouth and from the entrance to the constriction are x and z, respectively; the position of the splice point, d_s, is measured from the *left* hand entrance to the constriction.

Image Potential

A similar splicing procedure can be used to estimate the image potential in unsymmetrical channels. It is based on two observations:

(*a*) As an ion enters a pore, its electrical image is determined by the properties of the pore mouth. Until the ion has penetrated a substantial distance, a pore of finite length is functionally indistinguishable from one of infinite length (see Fig. 6 of the preceding paper).

(*b*) In the interior section of a pore, the whole ion-pore-membrane-water ensemble can be approximated as pore of uniform diameter spanning a somewhat thinner membrane. The effective pore length can be estimated from Eq. 14 of the preceding paper. This suggests that a splice point be chosen by separately symmetrizing the left- and right-hand sides of the ensemble and requiring that the peak in the image potential be the same for the two symmetrized halves. The potential to either side of the splice is that for the appropriate symmetrical system which insures that the potential is correct in the aqueous regions and near the entrances to the constriction. As the ion moves deeper into the narrow part of the channel, the approximation rests on the assumption that, divided in this way, the left- and right-hand sides of the system are electrostatically equivalent.

To illustrate the procedure, consider two examples of very unsymmetric systems with the geometry of Fig. 1 where $W = 5$ nm, L = 3 nm, and $R_R = 2$ nm ($R_L = 0$):

$$a_0 = 0.5 \text{ nm}, \quad \lambda = 6, \quad b_R = 4$$
$$a_0 = 0.2 \text{ nm}, \quad \lambda = 15, \quad b_R = 10.$$

A number of upper and lower bounds can be determined for the image potential $\Phi(z)$ by considering various symmetrization procedures,

$$\Phi_s(z; \beta, b) < \Phi(z) < \Phi_s(z; \lambda/2 + b, b) \qquad (1a)$$
$$\Phi_s(z; \lambda/2, 0) < \Phi(z) < \Phi_s(z; \beta, 0) \qquad (1b)$$

where $\beta = (\lambda + b)/2$ and Φ_s is the image potential of an ion in a symmetrical channel. In Eq. 1, coordinate axes are displaced so that the mouth of each substitute symmetrical pore is superposed on that of the model pore. The lower bounds correspond to symmetrized systems for which the membrane width is that of the model pore; for the upper bounds the constriction length in the symmetrized system is that of the model pore.

According to Eq. 14 of the preceding paper, pore mouths with radii $b = 4$ and 10 are equivalent to straight-sided segments of length ~1.96 and ~3.38, respectively. The interior sections of the two pores should be fairly well described by the geometries

$$\beta = 3.98, b = 0 \quad \text{or} \quad \beta = 6.02, b = 4$$
$$\beta = 9.19, b = 0 \quad \text{or} \quad \beta = 15.81, b = 10$$

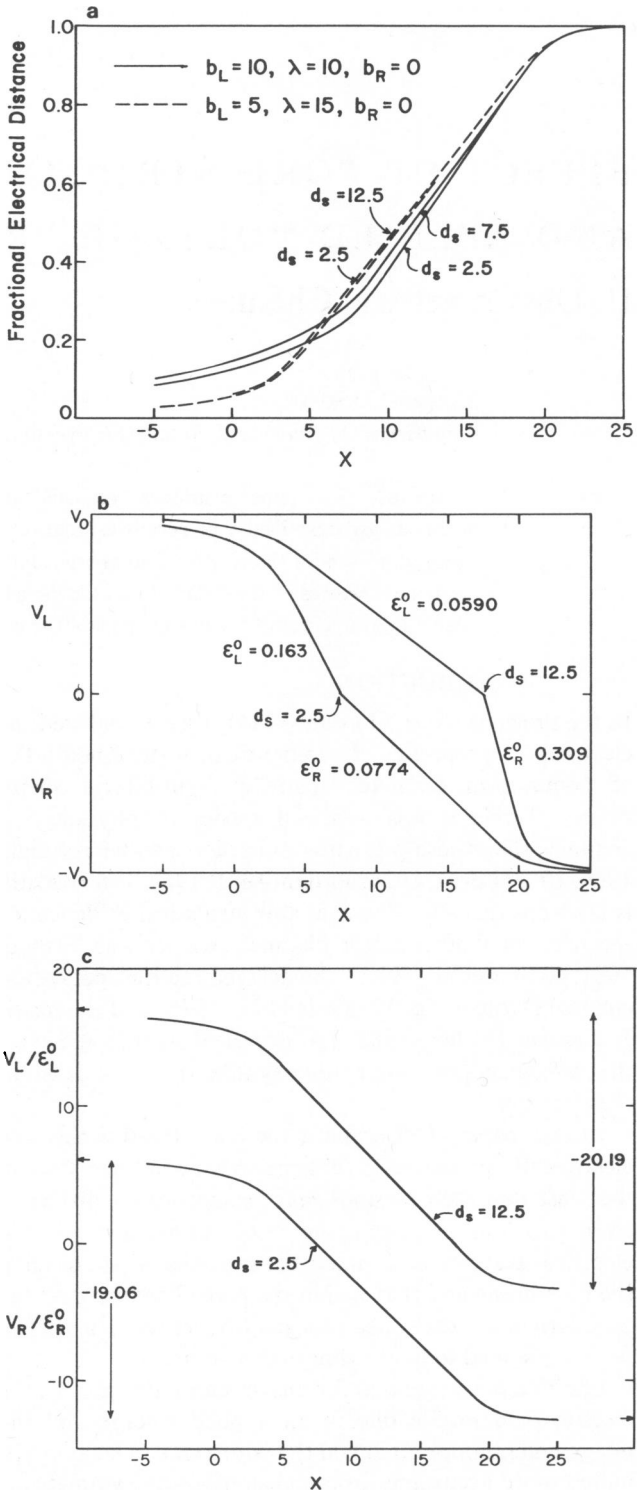

FIGURE 2 Splicing construction of the electrical distance profile for an ion in unsymmetrical pores with the geometry of Fig. 1. (*a*) Unscaled, unspliced potential profiles for a pore for which $b_L = 5, \lambda = 15$, and $b_R = 0$. Two splice points are contrasted. (*b*) Spliced profiles for the same pore geometry. The electric field in the constriction is constant but the potential profile is unscaled. (*c*) Electrical distance profiles for the same geometry and for a pore for which $b_L = 10, \lambda = 10$, and $b_R = 0$. The resultant profiles are only slightly dependent upon the choice of splice point.

Any $b = 0$ geometry yields the correct image potential for an ion near the left-hand mouth of the channel and any $b = 4$ (or 10) geometry is accurate near the right-hand mouth. Systems with β values near these should be equivalent when an ion is near the channel center. Thus, the potential maxima should be roughly at $z = 3.98$ and at $z = 9.19$. Because Eq. 14 of the preceding paper is approximate (there is some scatter in the data of Fig. 3 of the preceding paper), the actual maxima are slightly displaced. They occur at the scaled distances $z = 3.85$ and $z = 9.28$, respectively, i.e., at 1.93 and at 1.86 nm from the left-hand entrance to the channels.

The results are illustrated in Fig. 3. For most points in the channels there is very little difference between the bounds estimated from Eq. 1 or the curves calculated by the interpolation procedure described. The largest possible absolute error occurs in case 2 (Fig. 3 *b*) at a distance ~2.25 nm from the left-hand mouth; extrapolating the bounding curves (the potential has a unique maximum) suggests an absolute error of no more than ~5.6 kJ mol^{-1}, ~15%. In case 1 (Fig. 3 *a*) the error is greatest ~2.1 nm from the left-hand mouth. Extrapolation suggests an absolute error no greater than ~1.9 kJ mol^{-1}, ~21%. These uncertainties are most likely gross overestimates Fig. 5, *b–d*, of the preceding paper clearly demonstrates that as long as an ion has penetrated more than $2a_0$ into a channel mouth, the "effective pore length" approximation is accurate to better than 5%. Thus, the potential determined by splicing the narrow pore (Fig. 3 *b*) should be accurate for 0.4 nm $\leq x \leq$ 2.6 nm. Only between 2.6 and 3 nm is there residual uncertainty; as the potential is a smooth continuous function, the associated error must be insignificant, probably $\leq$5%. For a wider pore (Fig. 3 *a*) the interior region only extends from 1 to 2 nm; even accounting for smoothness and continuity there is considerable uncertainty in the value of Φ between 2 and 3 nm, possibly as much as ~15%. The associated absolute error is probably $\leq$1 kJ mol^{-1}.

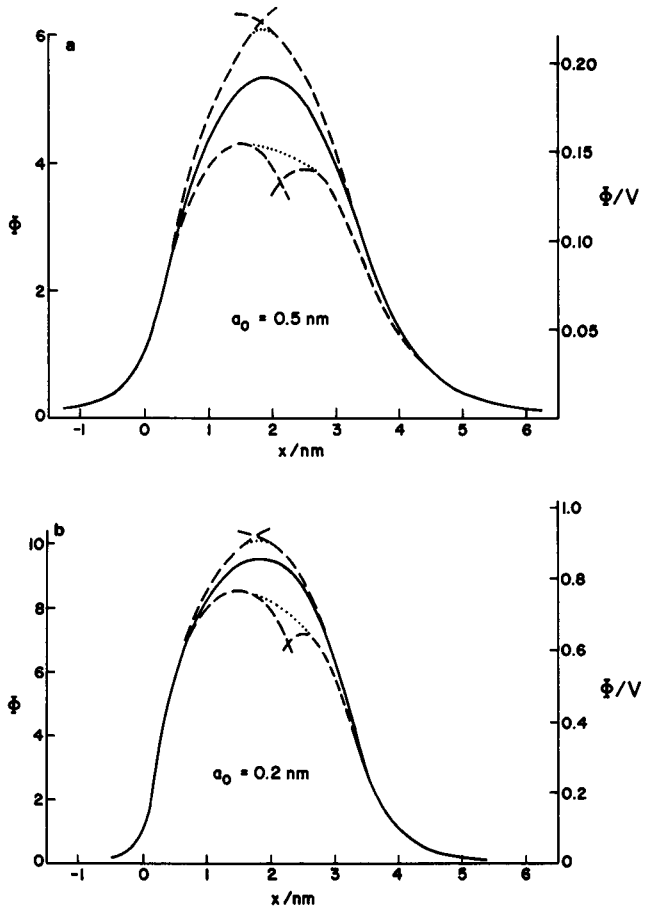

FIGURE 3 Image potential profiles of a monovalent ion estimated for two unsymmetrical model pores with the gross geometry of Fig. 1 where W = 5 nm, L = 3 nm, and R_R = 2 nm (R_L = 0). In *a* the channel is wide, a_0 = 0.5 nm, and in *b* it is narrow, a_0 = 0.2 nm. The dielectric constants are appropriate to the lipid water system, $\epsilon_1 = 80$, $\epsilon_2 = 2$. On the *left* axis the potential is measured in reduced units $e/\epsilon_1 a_0$ and on the *right* axis it is given in volts. The solid curves (___) correspond to the splicing procedure discussed in the text. The dashed curves (----) are upper and lower bounds to the true potential (see Eq. 1). The dotted lines (...) represent extrapolation of the bounding curves so that they are smooth and exhibit single maxima.

DISCUSSION

It is clearly advantageous to be able to estimate properties of unsymmetrical channels from those of symmetrical ones. Calculations for a small number of symmetric geometries can be used to model the properties of a much larger group of unsymmetrical ones. As the systems of biophysical importance are usually highly unsymmetrical, we now have the capacity to study more realistic models without further computational effort.

Delayed Rectifier Potassium Channel

Selectivity and permeability studies of the K channel from squid giant axon suggest that it has a long narrow region, ~0.3 nm in diameter (Bezanilla and Armstrong, 1972; Hille, 1973). Blocking studies with a series of quaternary ammonium derivatives (Armstrong, 1975*a*; Swenson, 1981; French and Shoukimas, 1981) provide evidence for the existence of an exterior mouth, ~0.8 nm in diameter, particularly well suited to accomodating a hydrated potassium ion or the head group of a blocker (Armstrong, 1975*a,b*). The functional model consistent with these data is illustrated in Fig. 4; the length of the mouth and the structure of the constriction are unknown.

Blocking has been shown to occur at the same electrical position, ~15–20% of the total voltage drop, regardless of inhibitor size for head groups between 0.8 nm and 1.2 nm in diameter (French and Shoukimas, 1981; Swenson,

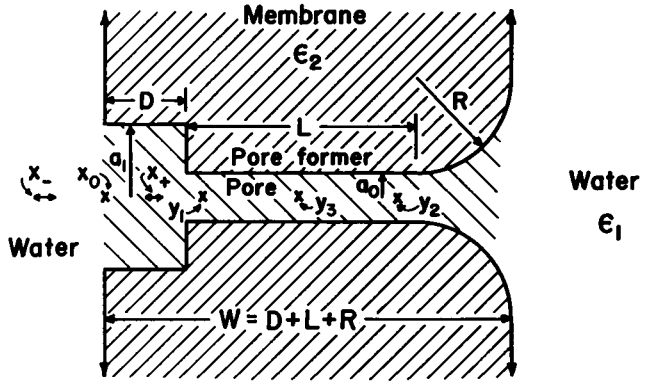

FIGURE 4 Model pore geometry that may bear some relation to the delayed rectifier potassium channel. The exterior mouth has a blocking region at x_+ (if blockers enter the mouth) or at x_- (if blockers can not enter the mouth). The mouth entrance is the point x_0. If this model pore has multiple binding sites the electrostatically favorable points are y_1 and y_2 (if there are two such sites) and also y_3 (if there are three such sites).

1981). Unless the exterior mouth is exceptionally long, the blocking site is only ~10% of the distance through the channel, and in the widest part of the system. Fractional electrical distance calculations indicate what mouth geometries account for both the electrical data and the structural model.

The channel is believed to "have at least three binding sites and often contain at least two ions at a time" (Hille and Schwartz, 1978). Ionic repulsion is quite significant in multiply occupied channels if the constriction length, L is short. Image potential calculations demonstrate why multiple occupancy may sometimes be a prerequisite for a channel to conduct.

Exterior Mouth Structure and Electrical Distance

Fractional electrical distances to sites in or near the channel mouth have been estimated for the model geometry of Fig. 4 by scaling. Table I lists the mouth size openings and constriction geometries treated; the membrane width varies between 4.8 and 5.5. nm. Pore mouth dimensions are compatible with the size of known blocking agents.

The different electrical radii accommodate various assumptions about the electrical and structural properties of the constriction. The smallest value, 0.15 nm, just permits K^+ passage and presumes the pore former is dielectrically equivalent to the lipid. The largest value, 0.25 nm, derives from assuming the pore forming region is quite polar, $\epsilon \sim 8$–12, and ~0.4 nm thick. The ϵ value, while high, is not unreasonable for polypeptides with polar side groups (Tredgold and Hole, 1976). The thickness is that of gramicidin A (Koeppe et al., 1978); it is about the smallest value consistent with a hydrophilic polar pore interior surrounded by lipophilic CH_2 groups. The electrical radius is then determined from shielding energy considerations (Jordan, 1981; 1983).

Electrical distances are calculated by splicing at the constriction entrance. This choice is not optimal; the plots of Fig. 2 *c* suggest that such an asymmetric splice may underestimate electrical distance in the mouth region. The associated errors could be as great as 15–20%.

Regardless of electrical geometry the external site x_- is only ~2/3 as far through the voltage drop as the interior site x_+. As the electrical position at which blocking occurs is independent of ion size for inhibitors as large or larger than $(C_2H_5)_4N^+$ (French and Shoukimas, 1981; Swenson, 1981), blocking occurs at the same physical position as well. Either the mouth is ~0.6 nm in radius, or the aliphatic groups of the larger blockers penetrate the structures forming the exterior mouth.

The electrical distance to the blocking site is very sensitive to the choice of electrical radius, as seen from Table II. An a_0 of ~0.15 nm is untenable even assuming the quoted values are as much as 20% low. The larger mouth sizes, $2.5 \leq D/a_1 \leq 3$, can account for the experimental observations as long as $a_0 > 0.2$ nm. The structural implications are that the mouth is between 1 and 1.2 nm long (if $a_1 = 0.4$ nm) and that the pore forming region is quite polar, $\epsilon \geq 6$, probably ~ 8–12.

Multiple Occupancy and Site Binding Energies

Electrical distance estimates are insensitive to the constriction length as long as $L + R$ is constant. The same is not true of the ionic repulsion energy in a multiply occupied channel. Decreasing L substantially increases the repulsion between ions bound at sites in the narrow region of the pore.

Electrically favorable tight binding sites are ones that are widely separated. For the model of Fig. 4, the optimal positions for a pair of sites are near y_1 and y_2; if a third site exists it should be in the middle, near y_3.

The single site binding energy, $\Delta\epsilon_i$, depends upon all forces that affect ion permeability. Structural perturbation may accompany binding. However, if multiple occupancy does not further alter channel structure, the ionic repulsion energy, U_{ij}, is determined by image forces alone. If double occupancy is observable, it is roughly as probable as single occupancy (and when triple occupancy is observable, it is roughly as probable as double occupancy); i.e., the total energy when two sites are filled is about the same as the

TABLE I
PARAMETERS USED IN MODELING THE ELECTRICAL BEHAVIOR OF CHANNEL ENSEMBLES WITH THE GEOMETRY SHOWN IN FIG. 4

Mouth sizes		Electrical radius	Constriction length
D/nm	a_1/nm	a_0/nm	*L/nm*
0.8	0.4	0.15	2.0
1.0	0.4	0.2	3.0
1.2	0.4	0.25	4.0
0.9	0.6		
1.2	0.6		
1.5	0.6		

These structures may have some relation to that of the delayed rectifier potassium channel. The distance $L_1 = L + R$ was held constant, $L_1 = 4$ nm. The membrane widths $W = L_1 + D = D + L + R$, varied from 4.8 to 5.5 nm.

TABLE II
FRACTIONAL ELECTRICAL DISTANCE TO THE BLOCKING REGION*

Mouth size	a_0/nm		
	0.15	0.2	0.25
Smaller (D/a_1 = 1.5-2)	0.06–0.08	0.07–0.12	0.09–0.14
Larger (D/a_1 = 2.5-3)	0.09–0.11	0.11–0.15	0.13–0.19

*For channels with the structure illustrated in Fig. 4 as a function of the electrical radius, a_0, for various mouth size openings.

energy when one site is occupied (or when three sites are filled, it is about the same as when two sites are occupied). The total energy for binding at sites i and j is

$$E_{ij}^{(2)} = \Delta\epsilon_i + \Delta\epsilon_j + U_{ij}. \quad (2)$$

It can be no greater than the binding energy for the most stable individual site. If the binding energies are ordered $\Delta\epsilon_1 < \Delta\epsilon_2 < \Delta\epsilon_3$, pair occupancy is most likely at sites 1 and 2. Because $E_{12}^{(2)} \leq \Delta\epsilon_1$, Eq. 2 yields the constraint $\Delta\epsilon_2 \leq -U_{12}$, which also implies that $\Delta\epsilon_1 < -U_{12}$. If triple occupancy occurs, the energetic consequences are stricter. The constraint is $E_{123}^{(3)} \leq E_{12}^{(2)}$ which implies that $\Delta\epsilon_3 \leq -U_{13} - U_{23}$. Other ordering patterns for the site binding energies yield different sets of bounds. The argument hinges upon only one assumption: structural changes due to multiple occupancy are the superposition of those due to binding at the individual sites.

The ionic repulsion energy in multiply occupied channels has been estimated by considering symmetrical pores with the constriction length and right-hand mouth structure of Fig. 4; the left-hand mouth has been modified. Repulsion energies were computed for occupancy at three points: $\pm(L/2 - 0.25$ nm), the analogues of y_1 and y_2, and the channel center, the analogue of y_3. While only approximate, this procedure provides an estimate of the effect that changing L, at constant $L + R$, has on the energetics of multiple occupancy.

For the replacement problem $\Delta\epsilon_1 = \Delta\epsilon_2$. Depending upon the value of $\Delta\epsilon_3$ pair occupancy occurs at sites 1 and 2 or at sites 1 (or 2) and 3. The bounds corresponding to different occupancy possibilities are

sites 1 and 2	$\Delta\epsilon_1 \leq -U_{12}$	(3a)
sites 1 (or 2) and 3	$\Delta\epsilon_3 \leq U_{12} - 2U_{13}$	(3b)
sites 1, 2 and 3	$\Delta\epsilon_3 \leq -2U_{13}$.	(3c)

The energies are listed in Table III as functions of a_0, L, and R. If multiple occupancy involves the interior site (y_3), the binding energy at the most stable site must be very large indeed, regardless of channel geometry.

Conductance, Constriction Length, and Multiple Occupancy

Bounds on the $\Delta\epsilon_i$ are significant because they are related to the rate constant for exiting a singly occupied channel. Comparison of these values with the off rate constants deduced from measurements of channel conductance indicate that electrostatic repulsion in a multiply occupied channel may greatly enhance its conductance.

The activation energy for channel conductance is essentially that for aqueous K^+ conductance (Frankenhauser and Moore, 1963). This energy, ~16 kJ mol^{-1}, is much less than most of the site binding energies tabulated. Andersen's (1983) treatment of the effect of aqueous diffusion on channel conductance indicates the conditions under which permeability can be diffusion limited even though individual steps have much higher activation barriers. As long as the single occupancy binding affinity is high, which is true if multiple occupancy is possible, the constraint is

$$k_- \gg 2\pi r_0 c D, \quad (4)$$

i.e., the rate of exiting the channel, k_-, is substantially larger than the capture rate, $2\pi r_0 c D$. Here k_- is the overall rate constant for exiting, r_0 the channel capture radius (Läuger, 1976), c the ion concentration, and D the aqueous diffusion coefficient. With an r_0 of ~0.03 nm, which describes the K^+ current in gramicidin (Andersen, 1983), k_- in 0.1 M K^+ must be greater than $\sim 1.5 \cdot 10^7$ s^{-1}.

Single channel conductance can also be used to estimate k_-. Viewing the channel as a set of series resistors, the conductance is approximately $(ze^2\alpha k_-)/k_BT$) where z is the valence of the permeant ion, e is the electronic charge, α is the voltage drop in the rate limiting step, and k_BT is Boltzmann's constant times temperature. Because the process is diffusion limited and entry into the exterior mouth is the diffusional process, α is the electrical position at which blocking occurs, i.e., $\alpha \sim 0.15$–0.20 (Swenson 1981; French and Shoukimas, 1981). Channel conductance is between 3 and 18 pS (Armstrong, 1971; Conti et al., 1975; Conti and Neher, 1980); k_- is therefore in the range $3 \cdot 10^6$–$2 \cdot 10^7$ s^{-1}, comparable with the capture rate estimate.

The theory of unimolecular rate processes provides theoretical estimates of the rate of exiting a singly occupied channel, k_-^0 (see Jordan, 1979); the result is $k_-^0 \sim 6 \cdot 10^{12} \exp(-\epsilon_-/k_BT)$. The barriers for exiting a singly occupied channel are no less than the largest value of $-\Delta\epsilon_i$; if rehydration upon exiting is not efficient, the overall barrier would be still greater. Thus $\epsilon_i \geq -\Delta\epsilon_i$ and bounds to k_-^0 are easily calculated. The results, listed in Table IV, contrast various multiple occupancy scenarios. As long as only the exterior sites (y_1 and y_2) are occupied,

TABLE III
UPPER BOUNDS TO THE MOST STABLE SINGLE SITE BINDING ENERGIES*

L/nm	R/nm	a_0/nm	Sites occupied (1,2) $\Delta\epsilon_i$	(1,3) $\Delta\epsilon_i$	(1,2,3) $\Delta\epsilon_i$
			(kJ mol^{-1})	(kJ mol^{-1})	(kJ mol^{-1})
4	0	0.15	− 2.4	−32	−34
3	1		−11.6	−66	−78
2	2		−30	−96	−126
4	0	0.2	− 2.4	−28	−30
3	1		−10.5	−53	−64
2	2		−25	−71	−96
4	0	0.25	− 2.4	−24	−26
3	1		− 9.4	−43	−52
2	2		−21	−55	−76

*For symmetrized channels roughly equivalent to the model channel of Fig. 4. The consequences of various occupancy possibilities are contrasted.

TABLE IV
UPPER BOUNDS TO SINGLE OCCUPANCY EXIT RATES*

L/nm	R/nm	a_0/nm	Sites occupied (1,2) k^0_-	(1,3) k^0_-	(1,2,3) k^0_-
			s^{-1}	s^{-1}	s^{-1}
4	0	0.15	$2\cdot10^{12}$	$2\cdot10^{7}$	$8\cdot10^{6}$
3	1		$6\cdot10^{10}$	$2\cdot10$	0.2
2	2		$4\cdot10^{7}$	$1\cdot10^{-4}$	$8\cdot10^{-10}$
4	0	0.2	$2\cdot10^{12}$	10^{8}	$4\cdot10^{7}$
3	1		$9\cdot10^{10}$	$3\cdot10^{3}$	$5\cdot10$
2	2		$3\cdot10^{8}$	3	$1\cdot10^{-4}$
4	0	0.25	$2\cdot10^{12}$	$5\cdot10^{8}$	$2\cdot10^{8}$
3	1		10^{11}	$2\cdot10^{5}$	$6\cdot10^{3}$
2	2		10^{9}	$2\cdot10^{3}$	0.4

*From symmetrized channels roughly equivalent to the model channel of Fig. 4. The consequences of various multiple occupancy possibilities are contrasted.

the exit rate constant from a singly occupied channel, k^0_-, is consistent with the value deduced from experiment; both singly and doubly occupied channels could contribute to the conductance. If an interior site (y_3) is involved the conclusions are unaltered as long as the constriction is long ($L \sim 4$ nm). If the constriction is short ($L \leq 3$ nm) the calculated values of k^0_- are incompatible with the experimental observation. Here singly occupied channels can not contribute to ion conductance. Ions only exit from multiply occupied channels; the electrostatic repulsions provide the driving force necessary to escape from sites at which the ions are very tightly bound.

Binding another cation externally (at x_+) has no significant effect on the multiple occupancy properties of the constriction. The extra repulsion energy is too small to meaningfully alter the bounds on $\Delta\epsilon_i$ or k^0_-.

Summary

Combining experimental evidence from blocking, permeability, and activation studies, and interpreting it in electrostatic terms, limits the possible physical and electrical properties of the delayed rectifier potassium channel. (*a*) If aliphatic groups or blocking agents can penetrate the exterior mouth of the channel, its dimensions may be as small as $D = 1.0$ nm, $a_1 = 0.8$ nm (see Fig. 4). If such penetration can not occur, the minimum size is $D = 1.5$ nm, $a_1 = 0.6$ nm. (*b*) The channel constriction is highly polar. Depending upon the physical radius of the constriction, the local dielectric constant is >6 and more likely between 8 and 12. (*c*) As long as only the exterior sites are occupied, both singly and doubly occupied channels can conduct even if L is as short as 2 nm. If the central site is occupied, only multiply occupied channels conduct unless the constriction is at least 4 nm long.

I wish to thank Christopher Miller and the referees for valuable criticism.

This research was partially supported by the National Institutes of Health grant GM-28643.

Received for publication 6 September 1983 and in final form 20 January 1984.

REFERENCES

Andersen, O. S. 1983. Ion movement through gramicidin A channels. Studies on the diffusion-controlled association step. *Biophys. J.* 41:147–165.

Armstrong, C. M. 1971. Interaction of tetraethylammonium ion derivatives with the potassium channels of giant axons. *J. Gen. Physiol.* 58:413–437.

Armstrong, C. M. 1975*a*. Ionic pores, gates and gating currents. *Q. Rev. Biophys.* 7:179–210.

Armstrong, C. M. 1975*b*. Potassium pores of nerve and muscle membrane. *In* Membranes. A Series of Advances. G. Eisenman, editor. Marcel Dekker, Inc., New York. 3:325–358.

Bezanilla, F., and C. M. Armstrong. 1972. Negative conductance caused by entry of sodium and cesium ions into the potassium channels of squid axons. *J. Gen. Physiol.* 60:588–608.

Conti, F., L. F. DeFelice, and E. Wanke. 1975. Potassium and sodium ion current noise in the membrane of the squid giant axon. *J. Physiol. (Lond.).* 248:45–82.

Conti, F., and E. Neher. 1980. Single channels recordings of K^+ currents in squid axons. *Nature (Lond.).* 285:140–143.

Frankenhauser, B., and T. E. Moore. 1963. The effect of temperature on the sodium and potassium permeability changes in myelinated nerve fibers of *Xenopus laevis*. *J. Physiol. (Lond.).* 169:431–437.

French, R. J., and J. J. Shoukimas. 1981. Blockage of squid axon potassium conductance by internal tetra-*N*-alkylammonium ions of various sizes. *Biophys. J.* 34:271–291.

Hille, B. 1973. Potassium channels in myelinated nerve. Selective permeability to small cations. *J. Gen. Physiol.* 61:669–686.

Hille, B. 1975. Ionic selectivity of Na and K channels of nerve membranes, *In* Membranes. A Series of Advances. G. Eisenman, editor. Marcel Dekker, Inc. New York. 3:255–323.

Hille, B., and W. Schwartz. 1978. Potassium channels as multi-ion single-file pores. *J. Gen. Physiol.* 72:409–442.

Jordan, P. C. 1979. Chemical Kinetics and Transport. Plenum Publishing Corp., New York, 293–298.

Jordan, P. C. 1981. Energy barriers for the passage of ions through channels. Exact solution of two electrostatic problems. *Biophys. Chem.* 13:203–212.

Jordan, P. C. 1982. Electrostatic modeling of ion pores. Energy barriers and electric field profiles. *Biophys. J.* 39:157–164.

Jordan, P. C. 1983. Electrostatic modeling of ion pores. II. Effects attributable to the membrane dipole potential. *Biophys. J.* 41:189–195.

Jordan, P. C. 1984. The effect of pore structure on energy barriers and applied voltage profiles I. Symmetrical channels. *Biophys. J.* 45:1091–1100.

Kistler, J., and R. M. Stroud. 1981. Crystalline arrays of membrane-bound acetylcholine receptor. *Proc. Natl. Acad. Sci. USA.* 78:3678–3682.

Kistler, J., R. M. Stroud, M. W. Klymkowsky, R. A. Lalancette, and R. H. Fairclough. 1982. Structure and function of an acetycholine receptor. *Biophys. J.* 37:371–383.

Koeppe, R. E., K. O. Hodgson, and L. Stryer. 1978. Helical channels in crystals of gramicidin A and of a cesium-gramicidin A complex: an x-ray diffraction study. *J. Mol. Biol.* 121:41–54.

Latorre, R., C. Vergara, and J. Hidalgo. 1982. Reconstitution in planar lipid bilayers of a Ca^{2+}-dependent K^+ channel from transverse tubule

membranes isolated from rabbit skeletal muscle. *Proc. Natl. Acad. Sci. USA.* 79:805–809.

Läuger, P. 1976. Diffusion-limited ion flow through pores. *Biochim. Biophys. Acta.* 455:493–509.

Levitt, D. G. 1978. Electrostatic calculations for an ion channel. I. Energy and potential profiles and interactions between ions. *Biophys. J.* 22:209–219.

Miller, C. 1982. *Bis*-quaternary ammonium blockers as structural probes of the sarcoplasmic reticulum K^+ channel. *J. Gen. Physiol.* 79:869–891.

Parsegian, V. A. 1969. Energy of an ion crossing a low dielectric membrane: solution to four relevant electrostatic problems. *Nature (Lond.).* 221:844–846.

Parsegian, V. A. 1975. Ion-membrane interactions as structural forces. *Ann. NY Acad Sci.* 264:161–174.

Swenson, R. P., Jr. 1981. Inactivation of potassium current in squid axon by a variety of quaternary ammonium ions. *J. Gen. Physiol.* 77:255–271.

Tredgold, R. H., and P. N. Hole. 1976. Dielectric behavior of dry synthetic polypeptides. *Biochim. Biophys. Acta.* 443:137–142.